

Electromagnetic Production of Pion Pairs*

CLAYTON D. ZERBY

Oak Ridge National Laboratory,† Oak Ridge, Tennessee

(Received June 19, 1961)

The Pauli-Weisskopf theory of pion pair production by photons was modified to include the strong pion-nucleus interaction in the form of a complex optical potential, and the matrix element was obtained by using "exact" distorted plane waves which were expanded into angular momentum eigenstates. Numerical calculations were performed for lead to examine the effect of a nuclear charge distribution and nuclear optical potential on the cross section in the energy region just above threshold. The calculations show that when the charge distribution and nuclear potential are included, the cross section for lead which leaves the nucleus in an unexcited state increases slowly just above threshold until approximately 295 Mev, where it starts to increase almost linearly, attaining a value of 1.07×10^{-22} cm² at 310 Mev.

I. INTRODUCTION

RECENTLY the Pauli-Weisskopf¹ theory of pion pair production by photons has been modified by Pomeranchuk² and Vdovin³ to include the strong pion-nucleus interaction in the form of an optical model. Whereas Pomeranchuk simply treated the nucleus as a black sphere, Vdovin permitted nuclear transparency and used the optical model of Fernbach *et al.*⁴ In both cases the problem was restricted to photon energies well above threshold and the electrostatic interaction was neglected.

The purpose of this work was to calculate the cross section for pion pair production by photons in the energy region just above threshold which is presently attainable, and to perform the calculations as accurately as possible. To achieve this objective it was necessary to represent the nucleus as a complex potential (optical model) in the equations of motion of the pions together with the modified Coulomb potential of the nucleus. In this case the interaction between the pion and radiation field was treated as the only perturbation and the field variables of the pion field were expanded in a series of "exact" distorted plane waves.

Some care had to be taken when the complex potential was introduced into the field-theoretical equations since it introduces dissipation into a theory whose framework is essentially nondissipative (dissipation as used here is meant to refer to the absorption of particles and energy in a continuous, unquantized manner). The problem is particularly acute in the case of pair production by photons since one must be assured that the optical potential enters the equations in such a way as to obtain dissipation (absorption) of both π^+ and π^- mesons, since they enter the theory in a symmetric way.

* Submitted to the University of Tennessee in partial fulfillment of the degree of Doctor of Philosophy.

† Operated by Union Carbide Corporation for the U. S. Atomic Energy Commission.

¹ W. Pauli and V. Weisskopf, *Helv. Phys. Acta* **7**, 709 (1934).

² Iu. Ia. Pomeranchuk, *Doklady Acad. Nauk S.S.S.R.* **96**, 265 and 481 (1954); also, *Proceedings of the Cern Symposium on High-Energy Accelerators and Pion Physics, Geneva 1956* (European Organization of Nuclear Research, Geneva, 1956) Vol. II, p. 167.

³ Yu. A. Vdovin, *Doklady Acad. Nauk. S.S.S.R.* **105**, 947 (1955).

⁴ S. Fernbach, R. Serber, and T. B. Taylor, *Phys. Rev.* **75**, 1352 (1949).

In Sec. II the method of introducing the optical potential into the field equations is discussed and it is shown that if the real part of the potential is treated as a world scalar and the imaginary part as the time component of a four-vector, it leads, in a consistent manner, to the scattering and absorption of the pions. The imaginary part of the potential leads to absorption and is intended to include, in a phenomenological way, all inelastic events that leave the nucleus in an excited state. It acts to remove pions that have been produced within the nucleus, which in effect reduces the cross section, in addition to facilitating the momentum transfer to the nucleus.

The presence of the complex potential in the equations of motion of the pion field leads to an ambiguity in the form of the final-state functions appearing in the matrix element. The usual requirement that the final-state function having the asymptotic form of a plane wave plus spherical converging wave^{5,6} can actually be satisfied by two alternate solutions of the equations of motion. The choice between them had to be made on physical grounds as discussed in Sec. III.

As a convenient means of calculating the cross section in the energy region just above threshold, the wave functions appearing in the matrix element were expanded into angular momentum eigenstates and the cross section expressed in this formalism. This development is shown in Sec. IV.

Finally, calculations for lead are presented in Sec. V which show the effects of introducing an optical potential and the modified Coulomb potential that results from assuming a charge distribution for the nucleus. The consideration of the charge distribution for the nucleus in this theory is necessitated by the fact that the pion pair production by photons takes place predominantly within the bounds of the nucleus in the energy region just above threshold.

II. INTRODUCTION OF THE OPTICAL POTENTIAL

For the purposes of discussing the proper form of the complex potential in the field equations, it is appro-

⁵ N. F. Mott and H. S. W. Massey, *The Theory of Atomic Collisions* (Oxford University Press, New York, 1949), 2nd ed., pp. 111 and 353.

⁶ G. Breit and H. A. Bethe, *Phys. Rev.* **93**, 888 (1954).

priate to introduce two real world scalars, P and P_1 , and the complex time component of a four-vector V_0 . At first, to display the covariance of the equations, all components of the four-vector will be shown; however, the space components will be taken to have the value zero when necessary. The natural units $\hbar=c=1$ are used except where noted to the contrary.

With the potentials present, the variation of the action can be patterned after the equation that appears in classical mechanics when nonconservative forces are present⁷:

$$\delta I = \delta \int \mathcal{L} d^4x + \int (Q\delta\phi + Q^*\delta\phi^*) d^4x = 0, \quad (2.1)$$

where

$$\mathcal{L} = -\frac{1}{2} \frac{\partial A_\mu}{\partial x_\nu} \frac{\partial A^\mu}{\partial x^\nu} - [(\mu+P)^2 - P_1^2] \phi^* \phi + \left(\frac{\partial}{\partial x^\mu} - ieA_\mu \right) \phi^* \left(\frac{\partial}{\partial x_\mu} + ieA^\mu \right) \phi, \quad (2.2)$$

and

$$Q = \left[\left(\frac{\partial}{\partial x^\mu} - ieA_\mu \right) V^{*\mu} + V_\mu^* \left(\frac{\partial}{\partial x_\mu} - ieA^\mu \right) - V_\mu^* V^{*\mu} + 2i(\mu+P)P_1 \right] \phi^*. \quad (2.3)$$

Certain terms in (2.3) can logically be included in the Lagrangian density and will lead to the same results below; however, for simplicity, because of the convenient notation, these terms are retained in the expression for Q .

Performing the variation indicated in (2.1) leads to the usual expression for the four-current⁸ and the following equation of motion for the pion field:

$$\partial \mathcal{L} / \partial \phi - (\partial / \partial x^\mu) (\partial \mathcal{L} / \partial \phi_\mu) + Q = 0. \quad (2.4)$$

With the aid of (2.2) and (2.3), (2.4) reduces to the equation satisfied by that field variable $\phi(\mathbf{r}, t)$. However, in order to display the equations that apply to the π^- and π^+ mesons, the equation satisfied by the Fourier transform $\psi(\mathbf{r}, \omega')$ of the field variable is obtained first, and a new frequency ω_k is defined so that $\omega_k = |\omega'|$. This results in the two equations,

$$\begin{aligned} & [(\omega_{k'} - eA_0 - iV_0)^2 + \nabla^2 \\ & - (\mu + P + iP_1)^2] \psi_{k'}(\mathbf{r}, \omega_{k'}) = 0, \end{aligned} \quad (2.5)$$

$$\begin{aligned} & [(\omega_{k''} + eA_0 + iV_0)^2 + \nabla^2 \\ & - (\mu + P + iP_1)^2] \psi_{k''}(\mathbf{r}, -\omega_{k''}) = 0, \end{aligned} \quad (2.6)$$

⁷ H. Goldstein, *Classical Mechanics* (Addison-Wesley Publishing Company, Inc., Reading, Massachusetts, 1953), p. 38.

⁸ S. S. Schweber, H. A. Bethe, and F. deHoffmann, *Mesons and Fields* (Row, Peterson and Company, Evanston, Illinois, 1955), Vol. I, p. 118.

which apply to the π^- and π^+ mesons, respectively, and where, in general, $\omega_k^2 = k^2 + \mu^2$.

Examination of (2.5) and (2.6) shows that the imaginary part of V_0 does not introduce a complex factor into the equations and therefore cannot introduce absorption. It can represent the real part of the optical potential however, although it enters the equations with opposite sign and will be an attractive potential for one of the pair of pions and repulsive for the other. In contrast to this, the potential P can represent the real part of the potential and appears in both equations with the same sign. Since experiments indicate that the real part of the potential should have the same sign and approximately the same magnitude for both π^+ and π^- , it can be assumed that the imaginary part of V_0 is very much smaller than P and, for simplicity, the imaginary part of V_0 will be set to zero in the subsequent development.

To proceed in the determination of whether V_0 (which is now real) or P_1 should represent the imaginary part of the potential, it should be noted that the Lagrangian density (2.2) is invariant to the transformation $\phi \rightarrow \phi e^{i\lambda} \cong (1+i\lambda)\phi$, where λ is a real infinitesimal constant. Therefore, under this transformation, the variation of \mathcal{L} must be zero.⁹ Performing the variation and using $\delta\phi = i\lambda\phi$ leads to the expression

$$-ie(Q\phi - Q^*\phi^*) = \partial j^\mu / \partial x^\mu = \nabla \cdot \mathbf{j} + \partial \rho / \partial t,$$

or

$$\nabla \cdot \mathbf{j} - 2V_0 \rho - 4e(\mu + P)P_1 \phi \phi^* + \partial \rho / \partial t = 0. \quad (2.7)$$

than V_0 since it introduces an absorptive term which is not proportional to the charge density. That is, if the charge and current density change sign, then the term containing V_0 maintains its absorptive properties whereas the term containing P_1 changes from an absorption to a production term. If P_1 is assumed to be zero, as is done in the subsequent work, then (2.7) reduces to the continuity equation which can be derived from the Schrödinger equation when a complex potential is present.¹⁰

Thus we find that when the imaginary part of the optical potential is treated as the time component of a four-vector and the real part as a world scalar, results are achieved which are consistent with elementary intuition as to the way in which positive and negative pions are treated by the nucleus.

III. FORM OF THE FINAL-STATE FUNCTION

The matrix element for pair production by photons is given by¹

$$M = -ie \int \mathbf{A}_q [\psi_{k''}^* \nabla \psi_{k'}^* - \psi_{k'}^* \nabla \psi_{k''}^*] d^3x, \quad (3.1)$$

⁹ S. S. Schweber, H. A. Bethe, and F. deHoffmann, *Mesons and Fields* (Row, Peterson and Company, Evanston, Illinois, 1955), Vol. I, Appendix B.

¹⁰ N. F. Mott and H. S. W. Massey, *The Theory of Atomic Collisions* (Oxford University Press, New York, 1949), 2nd ed., p. 12.

and it is assumed here, as it was by Vdovin,³ that this form applies when the imaginary part of the optical potential is introduced into the theory. The functions $\psi_{\mathbf{k}'}$ and $\psi_{\mathbf{k}''}$ that appear in (3.1) satisfy (2.5) and (2.6) where $P_1=0$ and V_0 is real.

It has been shown previously^{5,6} that the final-state continuum functions appearing in a matrix element should have the asymptotic form of a plane wave plus a spherical converging wave, $\psi_{\mathbf{k}^-}$. Usually this form is related to the function having the asymptotic form of a plane wave plus spherically diverging wave, $\psi_{\mathbf{k}^+}$, by the relation $\psi_{\mathbf{k}^-} = \psi_{\mathbf{k}^+}^*$. This occurs because of the assumption that the radial part of $\psi_{\mathbf{k}}$ and the phase shifts are real. In the present case, however, the complex coefficients occurring in the wave equation leads to complex radial functions and phase shifts, and the equality does not hold, so that a closer examination of the form of the final-state wave function is required.

In the following, the wave equation for the π^- meson will be examined explicitly and no generality will be lost if it is assumed that A_0 is zero. With the aid of (2.5) the equation satisfied by the radial function $R_l(r) = r^{-1}\chi_l(r)$ can be obtained from

$$\left\{ \frac{d^2}{dr^2} + \left[k^2 - 2\mu P - V_0^2 - P^2 - \frac{l(l+1)}{r^2} \right] - 2iV_0\omega_k \right\} \chi_l(r) = 0. \quad (3.2)$$

where $\chi_l(0)=0$ and $\chi_l(r) \sim \sin(kr - \frac{1}{2}l\pi + \eta_l)$, the term η_l being the complex phase shift. Thus the wave function $\psi_{\mathbf{k}}$ can be expanded as

$$\psi_{\mathbf{k}} = \sum_l A_l P_l(\mu) \frac{\chi_l(r)}{kr(2\omega_k)^{\frac{1}{2}}} \sim \sum_l A_l P_l(\mu) \frac{\sin(kr - \frac{1}{2}l\pi + \eta_l)}{kr(2\omega_k)^{\frac{1}{2}}}, \quad (3.3)$$

where \mathbf{k} is directed along the z axis and μ is the cosine of the polar angle. The factor $(2\omega_k)^{-\frac{1}{2}}$ has been introduced in (3.3) for proper normalization. By selecting $A_l = (2l+1)i^l \exp(-i\eta_l)$, $\psi_{\mathbf{k}}$ has the form $\psi_{\mathbf{k}^-}$. Whereas, if $A_l = (2l+1)i^l \exp(i\eta_l)$, then $\psi_{\mathbf{k}}$ has the form $\psi_{\mathbf{k}^+}$ (reference 11). To obtain $\psi_{-\mathbf{k}}$ from (3.3) it is only necessary to make the transformation $\mu \rightarrow -\mu$ and to note that $P_l(-\mu) = (-1)^l P_l(\mu)$.

Instead of examining the two possible forms of the final state functions, $\psi_{\mathbf{k}^-}$ and $\psi_{-\mathbf{k}^+}$ to resolve the problem as to which is correct, it is more appropriate to examine their complex conjugates since this is the form in which they would appear in the matrix element.

¹¹ L. D. Landau and E. M. Lifshitz, *Quantum Mechanics* (Addison-Wesley Publishing Company, Inc., Reading, Massachusetts, 1958), p. 397.

Thus we must consider the two alternate forms,

$$\psi_{\mathbf{k}^-} \sim \sum_l \frac{(2l+1)(-i)^l P_l(\mu)}{2ikr(2\omega_k)^{\frac{1}{2}}} \times [\exp(2i\eta_l^*) e^{i(kr - \frac{1}{2}l\pi)} - e^{-i(kr - \frac{1}{2}l\pi)}], \quad (3.4)$$

$$\psi_{-\mathbf{k}^+} \sim \sum_l \frac{(2l+1)(-i)^l P_l(\mu)}{2ikr(2\omega_k)^{\frac{1}{2}}} \times [\exp(2i\eta_l) e^{i(kr - \frac{1}{2}l\pi)} - e^{-i(kr - \frac{1}{2}l\pi)}], \quad (3.5)$$

which differ only in the way the phase shift enters the expressions. The one required will be the expression in which the square modulus of the amplitude of the outgoing spherical wave is less than that of the incoming spherical wave.

In (3.2) the imaginary part of the coefficient is positive since V_0 is a negative quantity. This leads to a phase shift which has a positive imaginary part and indicates $|\exp 2i\eta_l|^2 < 1$ and $|\exp 2i\eta_l^*|^2 > 1$. Therefore, it is clear that $\psi_{-\mathbf{k}^+}$ is the desired form of the final-state function for π^- mesons. A similar analysis based on (2.6) shows that $\psi_{\mathbf{k}^-}$ is the proper form for the π^+ mesons.

In the development of the two equations of motion for the π^- and π^+ mesons, the sign of the electronic charge e determines which equation applies to the π^+ or π^- meson. There is no *a priori* method of choosing the sign, since the equations are invariant to charge conjugation. Thus we have an additional check on the final waveforms by testing the invariance of the theory under the simultaneous transformation $e \rightarrow -e$, $\pi^+ \rightarrow \pi^-$, and $\pi^- \rightarrow \pi^+$, and indeed the choice of final waveforms meet the requirements.

IV. DEVELOPMENT OF THE CROSS SECTION IN ANGULAR MOMENTUM EIGENSTATES

The matrix element given in (3.1) was obtained with the use of the solenoidal gauge, $\nabla \cdot \mathbf{A} = 0$. This condition allows simplification of the matrix element since one of the terms in (3.1) can be converted into a surface integral over the infinite sphere plus a volume integral identical to the remaining term. The surface integral is easily shown to be zero and the matrix element becomes

$$M = -2ie \int \mathbf{A}_{\mathbf{q}}(\psi_{\mathbf{k}'}, \psi_{-\mathbf{k}^+}) \nabla \psi_{-\mathbf{k}^+} d^3x, \quad (4.1)$$

where

$$\psi_{-\mathbf{k}^+} = \sum_{l_1 m_1} \frac{4\pi(-i)^{l_1} \exp(i\eta_{l_1})}{k'r(2\omega_{k'})^{\frac{1}{2}}} \chi_{l_1} \times Y_{l_1, m_1}^*(\hat{k}') Y_{l_1, m_1}(\hat{r}), \quad (4.2)$$

and

$$\psi_{\mathbf{k}'^*} = \sum_{l_3} \frac{4\pi(-i)^{l_3} \exp(i\eta_{l_3}^*)}{k'r(2\omega_{k'})^{\frac{1}{2}}} \chi_{l_3} \times Y_{l_3, m_3}(\hat{k}'') Y_{l_3, m_3}^*(\hat{r}). \quad (4.3)$$

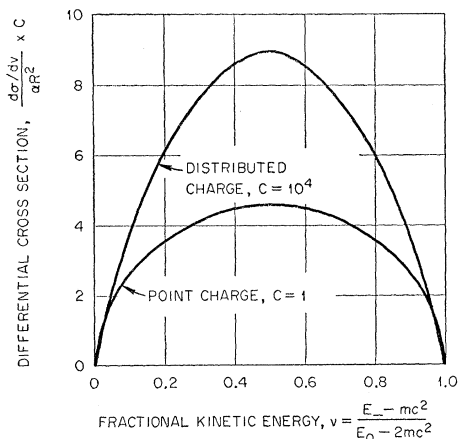


FIG. 1. Comparison of the Born approximation pion pair production cross section at a photon energy of 310 Mev for a point-charge and distributed-charge lead nucleus.

Equations (4.2) and (4.3) were obtained using the addition theorem for the Legendre polynomials so that \mathbf{k} has an arbitrary direction with respect to the axis of quantization.

The radial functions χ_{l_1} and $\chi_{l_3}^*$ in Eqs. (4.2) and (4.3) are obtained from the differential equations

$$\left\{ \frac{d^2}{dr^2} + \left[k'^2 - 2\omega_{k'} e A_0 - 2\mu P - V_0^2 - P^2 + e^2 A_0^2 - \frac{l_1(l_1+1)}{r^2} \right] - 2iV_0(\omega_{k'} + eA_0) \right\} \chi_{l_1} = 0, \quad (4.4)$$

$$\left\{ \frac{d^2}{dr^2} + \left[k''^2 + 2\omega_{k''} e A_0 - 2\mu P - V_0^2 - P^2 + e^2 A_0^2 - \frac{l_3(l_3+1)}{r^2} \right] - 2iV_0(\omega_{k''} - eA_0) \right\} \chi_{l_3}^* = 0, \quad (4.5)$$

with the boundary conditions such that at $r=0$ they have the value zero and asymptotically they have the form

$$\chi_{l_1} \sim \sin\left(k'r - \frac{1}{2}l_1\pi - \frac{\omega_{k'} Z\alpha}{k'} \ln(2k'r) + \eta_{l_1}\right), \quad (4.6)$$

and

$$\chi_{l_3}^* \sim \sin\left(k''r - \frac{1}{2}l_3\pi + \frac{\omega_{k''} Z\alpha}{k''} \ln(2k''r) + \eta_{l_3}^*\right). \quad (4.7)$$

In (4.1) there is considerable simplification if circularly polarized incident photons directed along the axis of quantization are used. With these conditions and the Rayleigh expansion of the plane wave, $\exp(iqz)$, the following expression is obtained¹²:

$$\mathbf{A}_q = -p\xi_p \frac{4\pi}{(2\omega_q)^{\frac{1}{2}}} \sum_{l_2} i^{l_2} (2l_2+1)^{\frac{1}{2}} j_{l_2}(qr) Y_{l_2,0}(\hat{r}), \quad (4.8)$$

¹² M. E. Rose, *Elementary Theory of Angular Momentum* (John Wiley & Sons, Inc., New York, 1957), p. 60.

where the factor $(4\pi/2\omega_q)^{\frac{1}{2}}$ is required for proper normalization. In (4.8) ξ_p is a spherical basis vector, and $p=+1$ and $p=-1$ corresponds to left and right circular polarization, respectively.

For unpolarized incident photons the differential cross section is given by

$$d\sigma = 2\pi \left(\frac{1}{2} \sum_{p=\pm 1} |M|^2\right) (2\pi)^{-6} k'' \omega_{k'} k' \omega_{k'} d\Omega' d\Omega d\omega_{k'}. \quad (4.9)$$

In order to obtain a workable expression for (4.9), it is necessary to reduce the expression for the matrix element. When (4.2) and (4.3) are inserted into (4.1) and the gradient formula¹³ is used, the matrix element becomes

$$M = \frac{-2iep(4\pi)^3}{k'k''(8\omega_q\omega_{k'}\omega_{k''})^{\frac{1}{2}}} \sum Y_{l_1, m_1}^*(\hat{k}') Y_{l_3, m_3}(\hat{k}'') \times I(l_1 l_2 l_3 L) J(l_1 l_2 l_3 L p m_1 m_3), \quad (4.10)$$

where the sum is over all possible values of the indicated quantum numbers. The functions I and J in (4.10) are given by

$$I(l_1 l_2 l_3 L) = i^{l_2} (-i)^{l_1+l_3} (2l_2+1)^{\frac{1}{2}} C(l_1 l_1 L; 00) \times \exp[i(\eta_{l_1} + \eta_{l_3}^*)] \int_0^\infty j_{l_2}(qr) \chi_{l_3}^* \times \left\{ \frac{d\chi_{l_1}}{dr} + \frac{1}{2} [l_1(l_1+1) - L(L+1)] \frac{\chi_{l_1}}{r} \right\} dr. \quad (4.11)$$

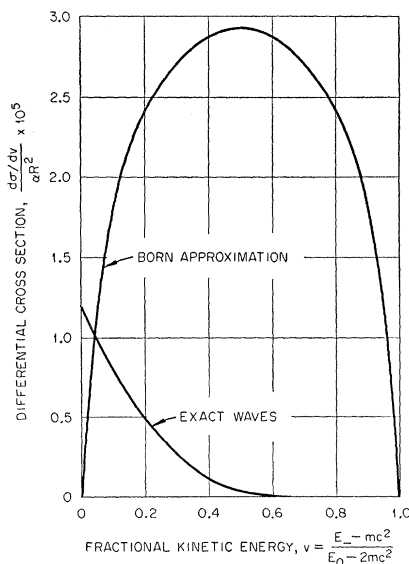


FIG. 2. Comparison of the Born approximation and exact wave pion pair production cross section for lead at a photon energy of 290 Mev. The nuclear potential was neglected.

¹³ M. E. Rose, *Elementary Theory of Angular Momentum* (John Wiley & Sons, Inc., New York, 1957), p. 124.

and

$$J(l_1 l_2 l_3 L p m_1 m_2) = \int Y_{l_3, m_3}^*(\hat{r}) Y_{l_2, 0}(\hat{r}) \xi_p \cdot \mathbf{T}_{l_1 L m_1} d\Omega, \quad (4.12)$$

where $C(l_1 1 L; 00)$ is a Clebsch-Gordan coefficient¹⁴ and $\mathbf{T}_{l_1 L m_1}$ is an irreducible tensor of rank L given by

$$\mathbf{T}_{l_1 L m_1} = \sum_{m_2} C(L 1 l_1; m_1 - m_2, m_2) \times Y_{L, m_1 - m_2}(\hat{r}) \xi_{m_2}. \quad (4.13)$$

After inserting (4.13) into (4.12) and noting that $\xi_p \cdot \xi_{m_2} = (-1)^p \delta(-m_2, p)$, the remaining integral over the product of three spherical harmonics can be readily performed¹⁵ yielding

$$J = (-1)^p \left[\frac{(2L+1)(2l_2+1)}{4\pi(2l_3+1)} \right]^{\frac{1}{2}} C(L 1 l_1; m_1 + p, -p) \times C(L l_2 l_3; m_1 + p, 0) \times C(L l_2 l_3; 00) \delta(m_3, m_1 + p). \quad (4.14)$$

The expression for the differential cross section (4.9) can now be put in a more desirable form by transforming to the variable $v = (\omega_{k'} - \mu)(\omega_q - 2\mu)^{-1}$ and inserting (4.10), (4.11), and (4.14) into (4.9) to get

$$d\sigma = \left(\frac{e^2}{\mu} \right) \left[\frac{8(1 - 2\mu/\omega_q)\mu^2 S}{k'' k' e^2} \right] dv d\Omega' d\Omega'. \quad (4.15)$$

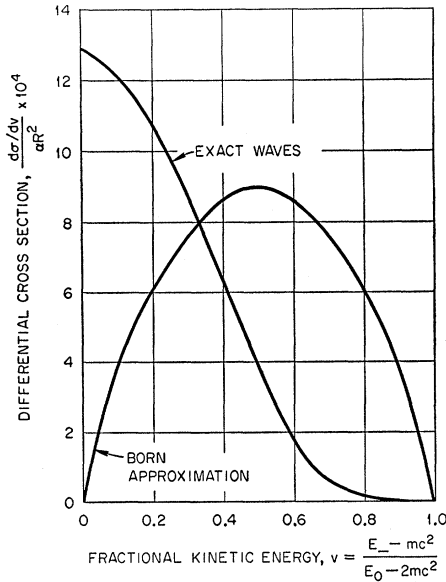


FIG. 3. Comparison of the Born approximation and exact wave pion pair production cross section for lead at a photon energy of 310 Mev. The nuclear potential was neglected.

¹⁴ The notation for the Clebsch-Gordan coefficient used here is that of M. E. Rose, *Elementary Theory of Angular Momentum* (John Wiley & Sons, Inc., New York, 1957).

¹⁵ M. E. Rose, *Elementary Theory of Angular Momentum* (John Wiley & Sons, Inc., New York, 1957), p. 62.

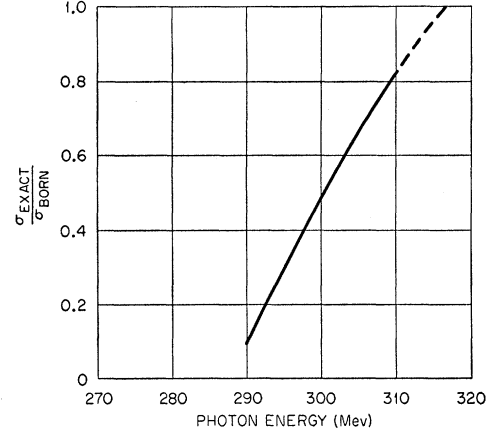


FIG. 4. Ratio of exact wave to Born approximation pion pair production cross section for lead as a function of photon energy. The nuclear potential was neglected.

The function S in (4.15) is given by

$$S = \sum C(L 1 l_1; m_1 + p, -p) C(L l_2 l_3; m_1 + p, 0) \times C(L' 1 l_1'; m_1' + p, -p) C(L' l_2' l_3'; m_1' + p, 0) \times I_1(l_1 l_2 l_3 L) I_1^*(l_1' l_2' l_3' L) Y_{l_1, m_1}(\hat{k}') Y_{l_1', m_1'}(\hat{k}') \times Y_{l_3, m_1 + p}(\hat{k}'') Y_{l_3', m_1' + p}(\hat{k}''),$$

where

$$I_1 = \left[\frac{(2L+1)(2l_2+1)}{(2l_3+1)} \right]^{\frac{1}{2}} C(L l_2 l_3; 00) I.$$

For purposes of the present problem the integration of S over all possible directions of \mathbf{k}'' and \mathbf{k}' is required, hence, we want to find the integral

$$K = \int \int S d\Omega' d\Omega''. \quad (4.16)$$

The integrals over the product of spherical harmonics appearing in (4.16) yields the product of four Kronecker delta symbols, $\delta(l_1, l_1') \delta(m_1, m_1') \delta(l_3, l_3') \delta(m_1 + p, m_1' + p)$, because of the orthogonality property of the functions, which permits the sum over l_1' , l_3' , and m_1' to be performed. Equation (4.16), therefore, reduces to

$$K = \sum V(LL'l_2 l_2' l_1 l_3) I_1(l_1 l_2 l_3 L) I_1^*(l_1 l_2' l_3' L'), \quad (4.17)$$

where

$$V(LL'l_2 l_2' l_1 l_3) = \sum_{m_1, (p=\pm 1)} C(L 1 l_1; m_1 + p, -p) C(L l_2 l_3; m_1 + p, 0) \times C(L' 1 l_1'; m_1 + p, -p) C(L' l_2' l_3; m_1 + p, 0). \quad (4.18)$$

It is possible to perform the sum in (4.18) by recoupling of the angular momenta. This is facilitated by noting that $L+L'$ and l_2+l_2' must be even. The

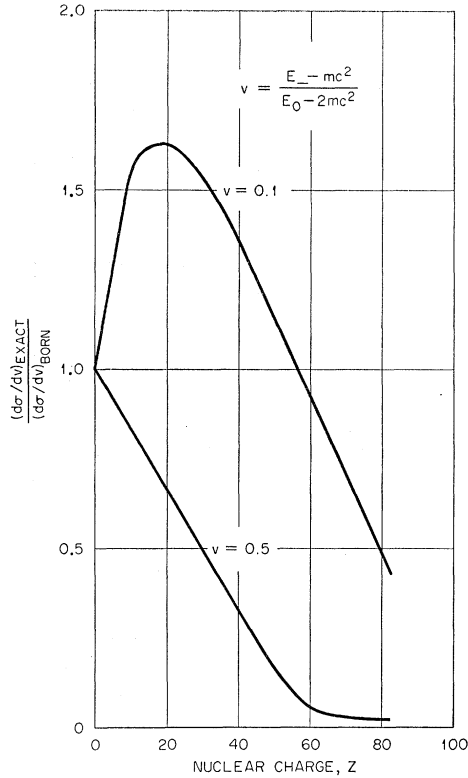


FIG. 5. Ratio of exact wave to Born approximation differential cross section as a function of Z for photon energy of 290 Mev.

recoupling yields

$$V(LL'l_2l_3) = \frac{2(2l_1+1)(2l_3+1)}{3(2l_2+1)(2L+1)} \delta(L, L') \delta(l_2, l_2') + (2l_1+1)(2l_3+1)(-1)^{l_2} \left(\frac{2}{3}\right)^{1/2} C(l_2' l_2 2; 00) \times W(L1L'1; l_1 2) W(2Ll_2' l_3; L'l_2), \quad (4.19)$$

where W is a Racah coefficient.

An additional simplification can be obtained by examining the product $I_1 I_1^*$ in (4.17). In that factor it is found that

$$I_1 I_1^* \propto (-i)^{l_1+l_3} (i)^{l_1+l_3} \times \exp[i(\eta_{l_1} + \eta_{l_3}^*)] \exp[-i(\eta_{l_1}^* + \eta_{l_3})], \quad (4.20)$$

so, if the real and imaginary parts of the phase shift are separated by letting $\eta_l = \alpha_l + i\delta_l$, then (4.20) becomes

$$I_1 I_1^* \propto \exp(-2\delta_{l_1}) \exp(+2\delta_{l_3}), \quad (4.21)$$

and it is seen that there is no need to obtain the real part of the phase shifts.¹⁶ With this development in mind and noting that K is a real quantity and that V is invariant to the simultaneous exchange of l_2 and L with l_2' and L' , respectively, then K can be written as

$$K = \sum Q(l_2 l_2' L L') V(LL'l_2 l_3) \times \text{Re} [G(l_1 l_2 l_3 L) G^*(l_1 l_2' l_3 L')], \quad (4.22)$$

¹⁶ From (4.4)–(4.7) it can be seen that $\delta_{l_1} > 0$ and $\delta_{l_3} < 0$, so both factors on the right of (4.21) are less than unity.

where

$$Q(l_2 l_2' L L') = \begin{cases} 1 & \text{if } l_2' = l_2 \text{ and } L' = L \\ 2 & \text{if } l_2' = l_2 \text{ and } L' < L \\ 2 & \text{if } l_2' > l_2 \\ 0 & \text{otherwise.} \end{cases}$$

and

$$G(l_1 l_2 l_3 L) = i^{l_2} \left[\frac{(2L+1)}{(2l_3+1)} \right] (2l_2+1) C(l_1 1 L; 00) \times C(LLl_3; 00) F(l_1 l_2 l_3 L),$$

in which

$$F(l_1 l_2 l_3 L) = \exp[-(\delta_{l_1} - \delta_{l_3})] \int_0^\infty j_{l_2}(qr) \chi_{l_3}^* \times \left\{ \frac{d\chi_{l_1}}{dr} + \frac{1}{2} [l_1(l_1+1) - L(L+1)] \frac{\chi_{l_1}}{r} \right\} dr.$$

Using (4.22), the final expression for the differential cross section becomes

$$d\sigma = (e^2/\mu)^2 [8(1 - 2\mu/\omega_q) \mu^2 K/k'' k' e^2] dv, \quad (4.23)$$

which was programmed for computation on an electronic computer.

V. CALCULATIONS OF THE CROSS SECTION

Since there is some interest in the effect on the value of the cross section as one goes from a point charge to distributed charge nucleus, this effect will be discussed first.¹⁷ To investigate this point it is advantageous to use the Born approximation differential cross section given by Pauli and Weisskopf¹⁸:

$$d\sigma = \frac{\pi e^4 |\Phi(p)|^2 P_+ P_- \sin\theta_- \sin\theta_+ d\theta_- d\theta_+ d\phi dE_-}{\hbar^5 c E_0^3 (2\pi)^4} (W), \quad (5.1)$$

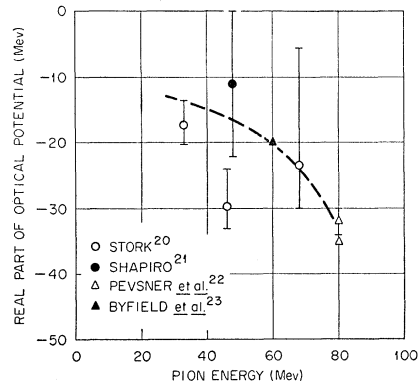


FIG. 6. Values of the real part of a square-well optical potential as determined from pion-nucleus scattering data.

¹⁷ In this section the equations will be given in ordinary units, where P is the momentum and E is the energy. The subscript $+$ and $-$ on a quantity indicates it is a variable for the π_+ and π_- mesons, respectively.

¹⁸ Equation (5.1) has been corrected by a factor of $\frac{1}{2}$ missing in the equation given in reference 1.

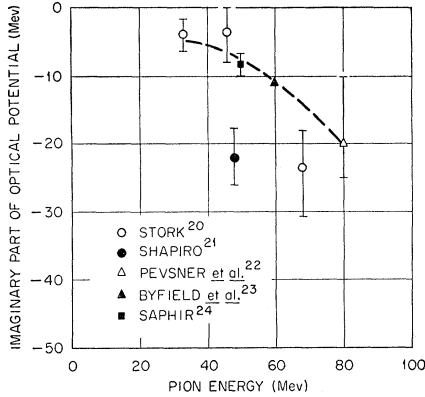


FIG. 7. Values of the imaginary part of a square-well optical potential as determined from pion-nucleus scattering data.

where

$$W = \frac{E_-^2 P_+^2 \sin^2 \theta_+}{(E_+ - cP_+ \cos \theta_+)^2} + \frac{E_+^2 P_-^2 \sin^2 \theta}{(E_- - cP_- \cos \theta_-)^2} + \frac{2E_+ E_- P_+ P_- \sin \theta_+ \sin \theta_- \cos \phi}{(E_+ - cP_+ \cos \theta_+)(E_- - cP_- \cos \theta_-)},$$

and

$$\Phi(\phi) = \int A_0(x) e^{i\mathbf{p} \cdot \mathbf{x}} d^3x.$$

In (5.1), $E_0 = E_+ + E_-$ and $\hbar\mathbf{p} = \mathbf{P} - \mathbf{P}_- + \mathbf{P}_+$, where $\hbar\mathbf{p}$ is the momentum transmitted to the nucleus and \mathbf{P} is the momentum of the photon.

For a point charge, $\Phi(\phi) = -4\pi eZ/p^2$, in which case (5.1) can be integrated to give

$$d\sigma = \alpha Z^2 \left(\frac{4}{3} R^2\right) \left(\frac{E_+ E_-}{P_+ c P_- c} L - 1\right) dE_-,$$

where $\alpha = e^2/\hbar c$ is the fine-structure constant, $R = e^2/mc^2$ is the classical pion radius, and

$$L = \ln \left| \frac{P_+ c P_- c + E_+ E_- + m^2 c^4}{-P_+ c P_- c + E_+ E_- + m^2 c^4} \right| = 2 \ln \left| \frac{P_+ c P_- c + E_+ E_- + m^2 c^4}{E_0 m c^2} \right|.$$

For the case of a distributed charge density, $Z\rho(r)$,

$$\Phi(\phi) = -\frac{4\pi Z e}{p^2} \int \rho(x) e^{i\mathbf{p} \cdot \mathbf{x}} d^3x. \quad (5.2)$$

and (5.1) has to be integrated numerically.

The cross section for lead ($Z=82$) was obtained from (5.1) for a charge density

$$\rho(r) = \frac{\rho_0}{1 + \exp[(r-b)/a]}, \quad (5.3)$$

which is reasonably close to the actual charge distribution for medium and heavy nuclei as obtained for electron scattering experiments.¹⁹ The constant ρ_0 is for normalization, and the constants a and b for best fit to experimental data are $a = 0.546 \times 10^{-13}$ cm and $b = 1.07 A^{1/3} \times 10^{-13}$ cm.

A comparison of the cross section with the charge distribution with that for a point-charge nucleus is shown in Fig. 1 for a photon energy of 310 Mev. The cross section is given in units of $\alpha R^2 = 7.762 \times 10^{-33}$ cm². The two curves have similar shapes, but the point-charge cross section is approximately a factor of 10^4 larger than that for the distributed charge. This factor persists in the energy range below 310 Mev.

A comparison of the cross section obtained with the exact wave calculation (4.23) with the Born approximation solution for a distributed charge is shown in Figs. 2 and 3. At the photon energies of 290 and 310 Mev, shown in the figures, a striking difference in the spectral shapes obtained from the two calculations will be noticed. The enhancement of the cross section for higher energy π^+ mesons is well known and occurs because of the repulsive Coulomb potential. The ratio of the total cross section obtained by the exact wave and Born approximation calculations is shown in Fig. 4.

The difference between the two calculations can be

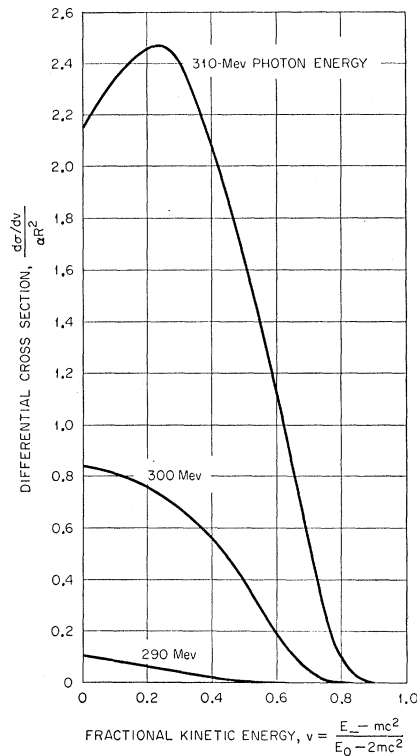


FIG. 8. The differential pion pair production cross section (by photons) for lead including the Coulomb and nuclear optical potential ($P = -16$ Mev, $V = -5$ Mev).

¹⁹ R. Hofstadter, Revs. Modern Phys. 28, 214 (1956).

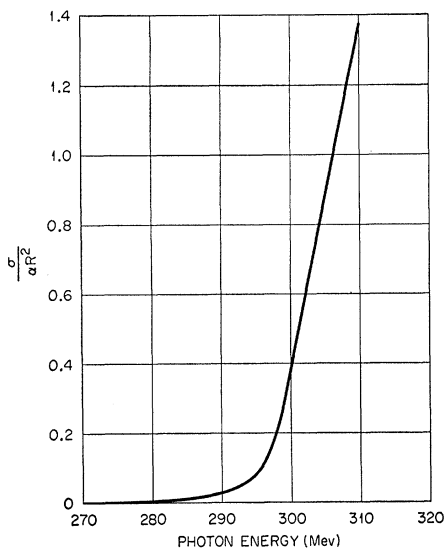


FIG. 9. The pion pair production cross section for lead including the Coulomb and nuclear optical potential ($P = -16$ Mev, $V = -5$ Mev) as a function of photon energy.

expected in the case just cited since the conditions for the Born approximation to hold, $Z\alpha E_+/P_+C$ and $Z\alpha E_-/P_-C \ll 1$, are certainly not obtained. It is of some interest then to see how the spectral shape of the exact wave solution approaches that of the Born approximation as $Z \rightarrow 0$. This also provides a badly needed check on the computational procedure. Figure 5 shows the ratio of the cross section for the exact wave solution to that of the Born approximation as a function of Z for $v=0.5$ and 0.1 at a photon energy of 290 Mev. In this comparison the extent of the charge distribution in (5.3) was kept constant; so the numbers refer to fictitious nuclei for $Z < 82$.

For the calculations with the nuclear optical potential the parameters for the well depths were obtained from pion scattering experiments²⁰⁻²⁴ and are shown in Figs. 6 and 7. The depth parameters for the real part of the potential shown in Fig. 6 had to be adjusted by the factor E/mc^2 to make them applicable to the present calculation, since it has been customary to introduce both the real and imaginary part of the potential as a time component of a four-vector in the analysis of pion scattering experiments (in contrast to the method discussed in Sec. II).

The potential parameters in the range 0-30 Mev pion energy were required in this calculation. The values selected were -16 Mev and -5 Mev for the real and imaginary part of the potential, respectively,

²⁰ D. H. Stork, Phys. Rev. **93**, 868 (1954).

²¹ A. M. Shapiro, Phys. Rev. **84**, 1063 (1951) and H. A. Bethe and R. R. Wilson, *ibid.* **83**, 690 (1951).

²² A. Pevsner *et al.*, Phys. Rev. **100**, 1419 (1955).

²³ H. Byfield, J. Kessler, and L. M. Lederman, Phys. Rev. **86**, 17 (1952).

²⁴ G. Saphir, Phys. Rev. **104**, 535 (1956).

and they were assumed to be constant.²⁵ The potential was taken as a square well with radius $1.4 A^{1/3} \times 10^{-13}$ cm and is typical of the value selected for analysis of pion scattering experiments.

The calculated differential cross section including the modified Coulomb potential and the nuclear optical potential are shown in Fig. 8. These data still show the effects of the Coulomb potential which tends to make the spectra unsymmetric about $v=0.5$, although the cross section has been considerably increased from the corresponding case without the optical potential. The data at 310 Mev shows a hump which can be accounted for on the basis that within the nuclear well the effective momentum of the pions is increased and the spectrum should be expected to tend towards the symmetric shape given by the Born approximation. Figure 9 presents the total cross section as a function of incident energy and indicates a sharp increase in the cross section about 15 Mev above threshold.

VI. DISCUSSION

Although the present calculation maintained at least 1% numerical accuracy throughout, a larger error no doubt occurred because of the uncertainty in the applicability of an optical potential which is independent of energy and in the optical potential parameters selected from the spread of experimental data. More data from pion-nucleus scattering experiments with improved methods of analysis would establish the potential parameters more accurately and ultimately lead to greater accuracy in calculations of the type described in this paper.

The strong pion-nucleus interaction, as characterized by the optical potential, is obviously very important to pion pair production by photons. Although the cross section is remarkably reduced in the energy region just above threshold as one considers the distributed charge nucleus in comparison with the point charge nucleus, this loss is fully regained by including the consideration of the optical potential. The increase in the cross section is very significant, putting the values in an experimentally interesting region especially for photon energies above 295 Mev.

Since the present calculation made no attempt to take the $\pi-\pi$ interaction into account, the experimental data might be expected to deviate from the spectral data presented in Fig. 8 beyond the obvious inaccuracies of the calculation. The onset of the interaction should be observed first at $v=0.5$ as the photon energy increases, since the pions have their greatest center-of-mass energy at this point. At the energies considered in this study, however, the c.m. energy of the pion pair is relatively low and well below the energy of the proposed resonance in the isotopic spin $t=1$

²⁵ The constancy of the potential parameters in the low-energy region is based on the multiple scattering analysis of R. M. Frank, J. L. Gammel, and K. M. Watson, Phys. Rev. **101**, 891 (1956), in which they took the nucleon motion into account.

state.²⁶ At these lower energies the $l=0$ interaction might be expected to dominate as pointed out by Carruthers and Bethe²⁷ and be observed first as the photon energy increases. In this connection, it should be noted that the produced pair of pions, as calculated here, is a mixture of $l=0, 1,$ and 2 isotopic spin states and is not restricted on the basis of charge parity arguments since all orders of interaction with the

²⁶ W. R. Frazer and J. R. Fulco, Phys. Rev. Letters **2**, 365 (1959).

²⁷ P. Carruthers and H. A. Bethe, Phys. Rev. Letters **4**, 536 (1960).

Coulomb field of the nucleus were taken into consideration.

ACKNOWLEDGMENTS

The author wishes to express his appreciation to Dr. T. A. Welton who suggested this problem and whose advice contributed markedly to every phase of this work. The continued encouragement of E. P. Blizard contributed to carrying this problem to completion and is gratefully acknowledged.

Radiative Modes of K -Meson Leptonic Decay*

DONALD E. NEVILLE†

Enrico Fermi Institute for Nuclear Studies, and Department of Physics, University of Chicago, Chicago, Illinois

(Received August 11, 1961)

The gamma-ray spectra for the decays $K \rightarrow \mu\nu\gamma$ and $K \rightarrow e\nu\gamma$ as well as $\pi \rightarrow \mu\nu\gamma$ and $\pi \rightarrow e\nu\gamma$ are calculated in full: Terms in the spectra proportional to lepton mass are retained so that the results are applicable to the muon decay mode, and the calculations take into account both inner bremsstrahlung radiation and radiation arising from structure in the meson vertex. The latter contributions are expressed in terms of two form factors.

The modes $K \rightarrow \mu\nu\gamma$ and $K \rightarrow e\nu\gamma$ can be used to test the validity of Wigner time-reversal invariance. Two ways of doing this are given, one based on measurements of the gamma spectra

and the other on measurements of the transverse polarization of the muons from the $K \rightarrow \mu\nu\gamma$ decay.

Calculations have been carried out on the effect of a possible intermediate vector boson on the decay $K \rightarrow e\nu\gamma$. The calculations are in substantial agreement with those of Kanazawa, Sugawara, and Tanaka (KST). Contributions from internal bremsstrahlung radiation, not calculated in KST, are given in the present paper. The strongly interacting intermediate states which give rise to structure-dependent radiation are listed, and a discussion of possible ambiguities in the KST test, arising from these states, is given.

I. INTRODUCTION

IN this paper, differential rates are calculated for the decay modes

$$\begin{aligned} K^\pm &\rightarrow \mu^\pm + \nu + \gamma, \\ K^\pm &\rightarrow e^\pm + \nu + \gamma, \end{aligned} \quad (1.1)$$

as well as for the decays in which the K meson is replaced by a pion. These results extend the calculations of earlier workers¹; in particular, the present calculations are applicable to the muon mode in (1.1) because all terms proportional to lepton mass are retained. The rates depend on photon energy, on the angle between photon and charged lepton (alternatively, on the kinetic energy of the charged lepton), on the known nonradiative decay lifetimes, and on two unknown functions of photon energy. Rates integrated over the angle are also given.

Electromagnetic and weak couplings are treated to first order in perturbation theory, while the effects of strong interactions are given without approximation in terms of form factors h_1 and h_2 .

* Work done under the auspices of the U. S. Atomic Energy Commission.

† National Science Foundation Predoctoral Fellow.

¹ S. A. Bludman and J. A. Young, Phys. Rev. **118**, 602 (1960); V. G. Vaks and B. L. Ioffe, Nuovo cimento **10**, 342 (1958). These papers contain further references.

Besides Lorentz and gauge invariance, it is assumed that the leptons couple to K mesons via the V and A variants (i.e., vector coupling with the two-component neutrino). This assumption seems reasonable because in the related K_{l2} processes (l =muon or electron),

$$\begin{aligned} K^\pm &\rightarrow \mu^\pm + \nu, \\ K^\pm &\rightarrow e^\pm + \nu, \end{aligned} \quad (1.2)$$

the muon mode of decay predominates. Just as in π_{l2} decay, such a result points to vector coupling.

The leptons are taken to couple "locally," with no particles mediating between the emission of the ν and charged lepton. As a consequence the form factors h_1 and h_2 for muon and electron modes in (1.1) are the same; therefore, such an assumption can be checked by measuring the $h_i(\mu)$ and $h_i(e)$ in turn and comparing results. In this manner several authors² have verified a local coupling hypothesis for the decays $\pi \rightarrow (2 \text{ leptons})$.

The complete expressions for the photon spectra of (1.1) are given in Sec. II, Eqs. (2.7) through (2.15), and the Appendix. Magnitudes of the various terms of the decay rates are discussed in Sec. III in connec-

² T. Fazzini, G. Fidecaro, A. W. Merrison, H. Paul, and A. V. Tollestrup, Phys. Rev. Letters **1**, 247 (1958); G. Impeduglia, R. Plano, A. Prodell, N. Samios, M. Schwartz, and J. Steinberger, *ibid.* **1**, 249 (1958).